ELSEVIER

Polymer 40 (1999) 1863–1870

polymer

# Multiple active sites model of ethylene polymerization with the $Cp_2ZrCl_2$–aluminoxanes catalytic system

Qi Wang[a,*], Jianhua Weng[a], Lin Xu[b], Zhiqiang Fan[a], Linxian Feng[a]

[a]*Department of Polymer Science and Engineering, Zhejian University, Hangzhou 310027, People's Republic of China*
[b]*Yanshan Research Institute of Petrochemical Technology, Beijing 102550, People's Republic of China*

Received 20 November 1997; revised 12 January 1998; accepted 13 April 1998

## Abstract

The kinetics of ethylene polymerization catalyzed by $Cp_2ZrCl_2$–different aluminoxanes was studied. More than one type of active site was presented in the polymerization reaction based on an analysis of the GPC curves. A multiple active sites kinetic model (MSmodel) was proposed. Good agreements in polymerization rate and variation of polydispersity were achieved for fitting the kinetic profiles with the MSmodel. © 1999 Elsevier Science Ltd. All rights reserved.

*Keywords:* $Cp_2ZrCl_2$–aluminoxanes; Ethylene polymerization; Kinetic model

## 1. Introduction

The discovery of homogeneous Ziegler–Natta catalytic systems comprising a metallocene and aluminoxane opened a new era in the world of polyolefins. New homo- and co-polymers have been prepared by changing the structure of the metallocene. The high activity of metallocene leads to its high value of commercial application. Compared with the wide study of the relationship between the structure of metallocene and the structure or properties of related products, the kinetics of metallocene catalysts have not been studied extensively.

Kaminsky and coworkers [1,2] reported that by varying the concentration of $Cp_2ZrCl_2$ and temperature the molecular weight may be adjusted and also reported that the lifetime of the catalyst is remarkably long. Schmid [3] also reported a large variation of the molecular weight with polymerization temperature. He attributed the effect of catalyst concentration on molecular weight to the change of Al/Zr ratio. Chien and Wang [4] proposed the first kinetic model for the polymerization of ethylene using the $Cp_2ZrCl_2$ catalyst system. The model assumes the presence of multiple active center types, chain transfer to methylaluminoxane (MAO), chain transfer to hydrogen, $\beta$-hydride chain transfer, one first-order deactivation reaction at 0°C and two first-order deactivation reactions at higher temperature. The average propagation rate constants for the various site types were estimated from productivity data and the experimentally determined number of active sites. The $\beta$-hydride chain transfer rate constants were estimated using number-average molecular weight data. The transfer to aluminum rate constants was estimated from metal–polymer bond concentration data, and the deactivation rate constants were estimated from polymerization rate data. In the Chien and Wang model no comparison between experimental and predicted polymerization rate and average molecular weights was made. Estrada and Hamielec [5] proposed another model for ethylene polymerization. The model includes the presence of two active site types with the gradual transition of one site type to the other. The polymerization rate data and molecular weight were measured for kinetic parameters estimation. The model-calculated average molecular weights and polydispersities agreed with the experimental data very well. The acceleration in polymerization rate from a value reached within the first 3 min of reaction time was also predicted by this model. In the Estrada and Hamielec model the fractions of polymers produced by two active site types which can be measured from GPC curves were not considered.

A simple approach was developed by Kissin [6] which provides a means to extract detailed molecular weight distribution (MWD) information from GPC data. Possible applications of the technique were demonstrated using several classes of linear polymers produced by radicals,

---

* Corresponding author.

0032-3861/99/$ - see front matter
PII: S0032-3861(98)00301-2

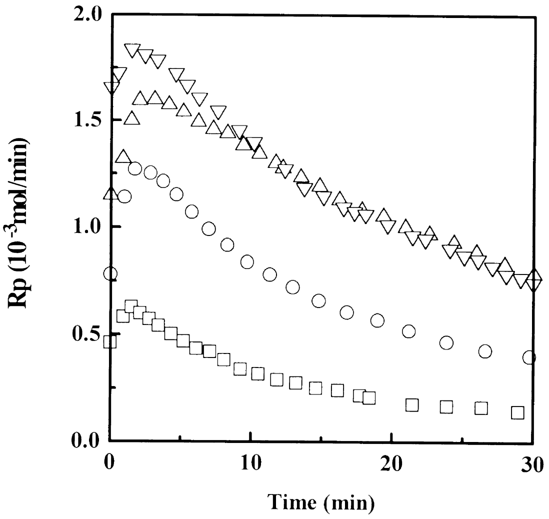

Fig. 1. Polymerization rate of different Al/Zr ratio with $Cp_2ZrCl_2$–MAO catalyst: □, Al/Zr = 2000; ○, Al/Zr = 4000; △, Al/Zr = 6500; ▽, Al/Zr = 10 000; [Zr] = 2.0 × $10^{-6}$ M; $T = 50°C$.

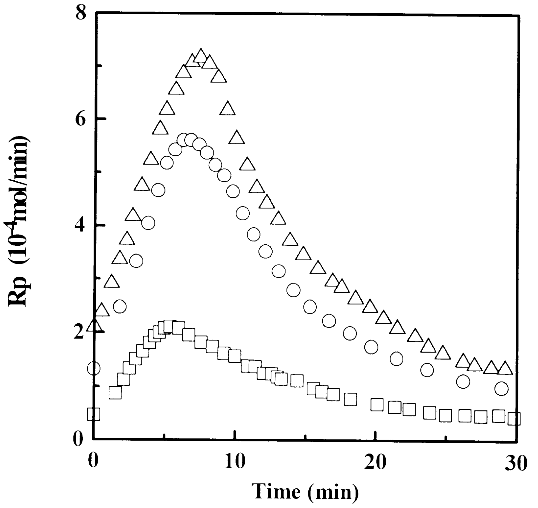

Fig. 2. Polymerization rate of different Al/Zr ratios with $Cp_2ZrCl_2$–BAO catalyst: □, Al/Zr = 5000; ○, Al/Zr = 7000; △, Al/Zr = 8000; [Zr] = 2.0 × $10^{-5}$ M; $T = 50°C$.

heterogeneous Ziegler–Natta catalysts and homogeneous metallocenes. Using this method, detailed information, such as number of active site types, fraction and molecular weights of the polymers produced by each active site, can be obtained from MWD analysis.

In this article a multiple active sites kinetic model (MSmodel) is proposed based on a combination of the kinetic models and the MWD analysis method described above. Ethylene polymerization using $Cp_2ZrCl_2$–MAO and BAO was simulated with the MSmodel and good agreements of polymerization rate, averaged molecular weights and variation of polydispersity were achieved.

## 2. Experimental procedure

### 2.1. Materials

MAO (Shering Co.), *iso*-$Bu_3Al$ (Aldrich Co.) and $Cp_2ZrCl_2$ (Fluka Co.) were used as received. Toluene was purified by refluxing over Na–K alloy under nitrogen atmosphere and distilled prior to use. BAO was prepared by hydrolysis of *iso*-$Bu_3Al$ with water in toluene at low temperature. Polymerization-grade ethylene was further purified by passing over 4 Å activated molecular sieves.

### 2.2. Polymerization procedure

The polymerization was carried out in a 100 ml glass autoclave equipped with ethylene inlet, magnetic stirrer and vacuum line. The autoclave was filled with 50 ml dry toluene and certain quantities of aluminoxane. The mixture was stirred at 30°C and then saturated with ethylene (1 atm). The reaction was initiated by adding the solution of $Cp_2ZrCl_2$ in toluene. After 30 min the polymerization was terminated by addition of acidified ethanol. The resulting polymer was separated by filtration and dried under vacuum until constant weight. The ethylene consumption was continuously recorded by magnetic valve. The stirring speed was 1500 rpm, at which the diffusion effect on polymerization was minimized.

### 2.3. Measurement

High temperature GPC was performed with a Waters 150C instrument at 135°C using four styragel ($10^3$, $10^4$, $10^5$, $10^6$ Å) pore size columns in series and *o*-dichlorobenzene as the solvent. Polystyrene was used for calibration.

## 3. Experimental results

### 3.1. Polymerization rate

Figs 1 and 2 show the polymerization rate data of ethylene catalyzed by $Cp_2ZrCl_2$–MAO and BAO. The maximum rate of polymerization is reached within a few minutes after introduction of metallocene and followed by the decay for both MAO and BAO systems. The polymerization rates of the BAO system decay more rapidly than those of MAO. It is noteworthy that there is a comparative long build-up period for BAO which can be attributed to its relative weak cocatalytic ability.

### 3.2. MWD

Figs 3 and 4 show the typical GPC curves of polyethylene produced by $Cp_2ZrCl_2$–MAO and BAO. For the MAO system the MWD is near 2.0, but for the case of BAO the MWD becomes wider and a shoulder peak (see the arrows in Fig. 4) is observed, which suggests that more than one active site is present. Using the approach proposed by Kissin [6],

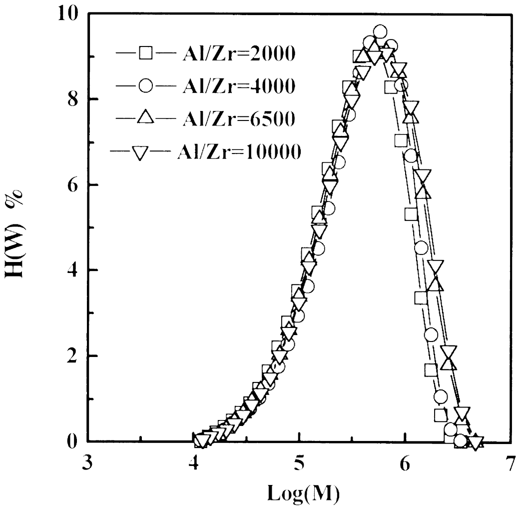

Fig. 3. GPC curves of polyethylene produced by $Cp_2ZrCl_2$–MAO catalyst using different Al/Zr ratios.

that is resolution of GPC curves using the Flory distribution equation, good results are achieved; these are illustrated in Figs 5 and 6. The GPC curves of polymer produced by MAO can be described by two Flory-distribution components with different molecular weights, whereas the GPC curves of BAO can be resolved into three components. Tables 1 and 2 give the detailed data. From the MWD analysis it can be concluded that there is more than one active site in both the MAO and BAO systems for various Al/Zr ratios. The Al/Zr ratio greatly affects the molecular weight and fraction of each component. With increasing Al/Zr ratio the molecular weight of each component improves and the fraction of high molecular weight component also increases.

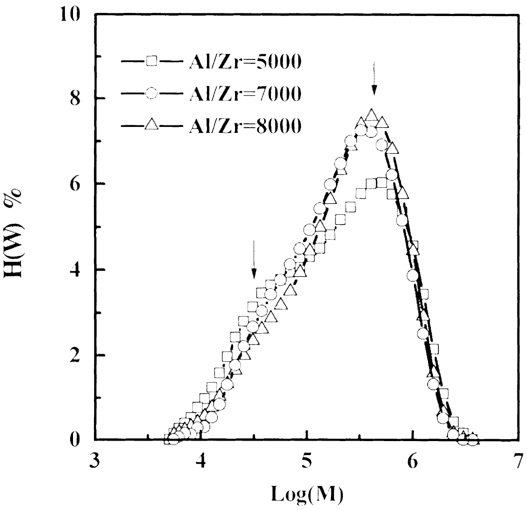

Fig. 4. GPC curves of polyethylene produced by $Cp_2ZrCl_2$–BAO catalyst using different Al/Zr ratios.

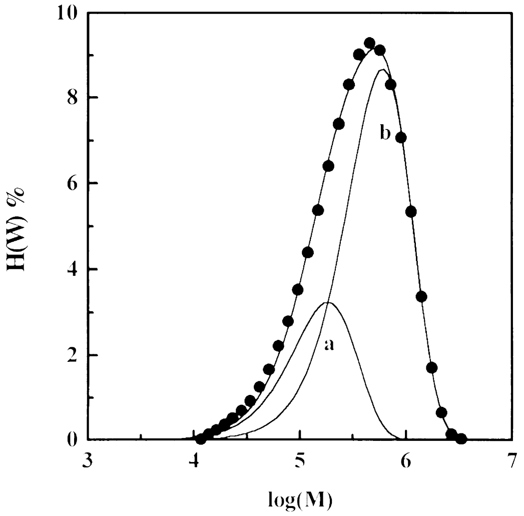

Fig. 5. Resolution for GPC curves of polyethylene prepared by $Cp_2ZrCl_2$–MAO (Al/Zr = 4000; dots: experimental data; lines: two Flory MWD functions and their sum).

### 3.3. Model development

The underlying assumptions made in the development of the model are: (1) instantaneous formation of sites of each type that produce different molecular weight polymers; (2) first-order propagation with monomer and active sites as generally believed; (3) first-order chain transfer to monomer; (4) first-order deactivation of each active site. Bimolecular deactivation is difficult to deal with and is therefore not considered.

With these assumptions, the polymerization reactions of a single site system can by described as follows according to law of mass action:

(a) instantaneous formation of active species

$$Cp_2ZrCl_2 + MAO + M \rightarrow R_1 \quad (1)$$

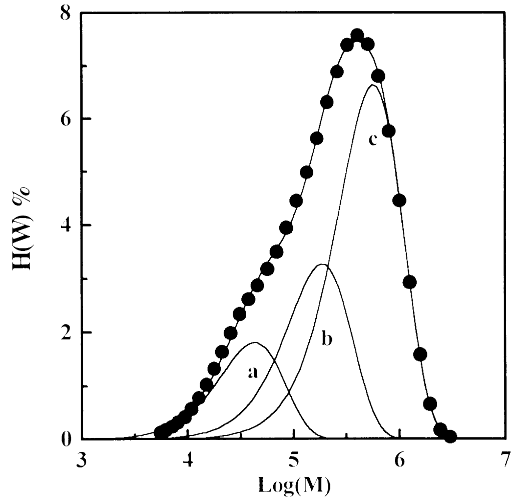

Fig. 6. Resolution for GPC curves of polyethylene produced by $Cp_2ZrCl_2$–BAO (Al/Zr = 7000; dots: experimental data; lines: three Flory MWD functions and their sum)

Table 1
Flory components in polyethylene prepared using $Cp_2ZrCl_2$–MAO with different Al/Zr ratios[a]

| Al/Zr | Flory distribution parameters |  | $M_n$ [d,e] | $M_w/M_n$ [e] |
|---|---|---|---|---|
|  | **a** | **b** |  |  |
| 2000 | 9.0[b]/27[c] | 29.6/73 | 32.0 | 2.64 |
| 4000 | 9.2/21 | 32.6/79 | 18.5 | 2.60 |
| 6500 | 12.0/37 | 42.4/63 | 20.2 | 2.94 |
| 10 000 | 12.2/36 | 44.8/64 | 20.5 | 3.06 |

[a] Polymerization conditions same as Fig. 1.
[b] $M_n$ of components ($10^4$ g mol$^{-1}$).
[c] Fraction of the component (wt%).
[d] $M_n$ of whole polymer ($10^4$ g mol$^{-1}$).
[e] Measured by GPC.

(b) propagation of active species

$$R_n + M \xrightarrow{k_p} R_{n+1} \tag{2}$$

(c) transfer to monomer

$$R_n + M \xrightarrow{k_{tr}} P_n + R_1 \tag{3}$$

(d) deactivation of active species

$$R_n \xrightarrow{k_d} P_n \tag{4}$$

where the $k$, $M$, $R_n$ and $P_n$ are the rate constants, the monomer, living polymer and dead polymer respectively. $R_n$ is living polymer with chain length $n$ and $P_n$ is the dead polymer produced from deactivation and chain transfer with chain length $n$.

The model equations may be written accordingly

$$\frac{dR_1}{dt} = -[(k_p + k_{tr})M + k_d]R_1 + k_{tr}M \sum_n R_n \tag{5}$$

$$\frac{dR_n}{dt} = -k_pMR_{n-1} - [(k_p + k_{tr})M + k_d]R_n \tag{6}$$

$$\frac{dP_n}{dt} = (k_{tr}M + k_d)R_n \tag{7}$$

The above equations can also be rewritten as

$$\frac{d\sum R_n}{dt} = -k_d \sum R_n \tag{8}$$

$$\frac{d\sum P_n}{dt} = (k_{tr}M + k_d) \sum R_n \tag{9}$$

The polymerization rate may be given by Eq. (10) if the monomer consumption of the initiation and transfer reaction is neglected.

$$R_p = \frac{dM}{dt} \approx k_pM \sum R_n \tag{10}$$

Table 2
Flory components in polyethylene prepared using $Cp_2ZrCl_2$–BAO with different Al/Zr ratios[a]

| Al/Zr | Flory distribution parameters |  |  | $M_n$ [d,e] | $M_w/M_n$ [e] |
|---|---|---|---|---|---|
|  | **a** | **b** | **c** |  |  |
| 5000 | 2.0[b]/23[c] | 8.6/28 | 32.8/49 | 6.64 | 5.77 |
| 7000 | 2.1/19 | 9.1/31 | 28.0/50 | 8.43 | 4.40 |
| 8000 | 2.5/15 | 9.8/28 | 28.0/57 | 8.88 | 3.85 |

[a] Polymerization conditions same as Fig. 2.
[b] $M_n$ of components ($10^4$ g mol$^{-1}$).
[c] Fraction of the component (wt%).
[d] $M_n$ of whole polymer ($10^4$ g mol$^{-1}$).
[e] Measured by GPC.

The moments of propagation polymer ($L$) and dead polymer ($J$) are respectively defined as

$$L_0 = \sum_n R_n; \quad L_1 = \sum_n nR_n; \quad L_2 \sum_n n^2R_n \tag{11}$$

$$J_0 = \sum_n P_n; \quad J_1 = \sum_n nP_n; \quad J_2 = \sum_n n^2P_n \tag{12}$$

$$\text{and } fS_0 = L_0 + J_0; S_1 = L_1 + J_1; S_2 = L_2 + J_2; \tag{13}$$

Thus the moments equations can be described as follows with long chain approximation.

$$\frac{dL_0}{dt} = -k_dL_0 \tag{14}$$

$$\frac{dL_1}{dt} = (k_p + k_{tr})ML_0 - (k_{tr}M + k_d)L_1 \tag{15}$$

$$\frac{dL_2}{dt} = (k_p + k_{tr})ML_0 + 2k_pML_1 - (k_{tr}M + k_d)L_2 \tag{16}$$

$$\frac{dJ_0}{dt} = (k_{tr}M + k_d)L_0 \tag{17}$$

$$\frac{dJ_1}{dt} = (k_{tr}M + k_d)L_1 \tag{18}$$

$$\frac{dJ_2}{dt} = (k_{tr}M + k_d)L_2 \tag{19}$$

The initial ($t = 0$) conditions can be summarized as follows:

$$R_1 = L_0 = L_1 = L_2 = C_0 \tag{20}$$

$$R_i = 0 \quad (i > 1) \tag{21}$$

$$P_i = J_n = 0 \quad (i > 1) \tag{22}$$

where $C_0$ is the initial mole mass of active species.

Eqs. (8) and (9) can be solved to give

$$\sum_n R_n = C_0\, e^{-k_dt} \tag{23}$$

$$R_p = k_pMC_0\, e^{-k_dt} \tag{24}$$

Integration of Eq. (24) leads to the expression of cumulative productivity $P$

$$P(t)=\int R_{\mathrm{p}}\,\mathrm{d}t=\frac{k_{p}MC_{0}}{k_{\mathrm{d}}}(1-\mathrm{e}^{-k_{\mathrm{d}}t}) \tag{25}$$

Eqs. (14)–(19) can be solved separately to give

$$L_0=C_0\,\mathrm{e}^{-k_{\mathrm{d}}t} \tag{26}$$

$$L_1=\frac{AC_0}{B-k_{\mathrm{d}}}(\mathrm{e}^{-k_{\mathrm{d}}t}-\mathrm{e}^{-Bt}) \tag{27}$$

$$L_2=\frac{AC_0}{(B-k_{\mathrm{d}})^2}(2k_{\mathrm{p}}M+B-k_{\mathrm{d}})(\mathrm{e}^{-k_{\mathrm{d}}t}-\mathrm{e}^{-Bt}) - \frac{2AC_0k_{\mathrm{p}}M}{B-k_{\mathrm{d}}}\,t\,\mathrm{e}^{-Bt} \tag{28}$$

$$J_0=\frac{BC_0}{k_{\mathrm{d}}}(1-\mathrm{e}^{-k_{\mathrm{d}}t}) \tag{29}$$

$$J_1=\frac{ABC_0}{B-k_{\mathrm{d}}}\left(\frac{\mathrm{e}^{-Bt}}{B}-\frac{\mathrm{e}^{-k_{\mathrm{d}}t}}{k_{\mathrm{d}}}-\frac{1}{B}+\frac{1}{k_{\mathrm{d}}}\right) \tag{30}$$

$$J_2=\frac{ABC_0(2k_{\mathrm{p}}M+B-k_{\mathrm{d}})}{(B-k_{\mathrm{d}})^2}\left(\frac{\mathrm{e}^{-Bt}}{B}-\frac{\mathrm{e}^{-k_{\mathrm{d}}t}}{k_{\mathrm{d}}}+\frac{1}{k_{\mathrm{d}}}-\frac{1}{B}\right) + \frac{2AC_0k_{\mathrm{p}}M}{B-k_{\mathrm{d}}}\left(\frac{\mathrm{e}^{-Bt}}{B}+t\,\mathrm{e}^{-Bt}-\frac{1}{B}\right) \tag{31}$$

$$S_0=C_0\left[\frac{B-k_d}{k_{\mathrm{d}}}(1-\mathrm{e}^{-k_{\mathrm{d}}t})+1\right] \tag{32}$$

$$S_1=\frac{AC_0}{k_{\mathrm{d}}}(1-\mathrm{e}^{-k_{\mathrm{d}}t}) \tag{33}$$

$$S_2=\frac{AC_0}{k_{\mathrm{d}}}\left(\frac{2k_{\mathrm{p}}M}{B-k_{\mathrm{d}}}+1\right)(1-\mathrm{e}^{-k_{\mathrm{d}}t})+\frac{2AC_0k_{\mathrm{p}}M}{B(B-k_{\mathrm{d}})}(\mathrm{e}^{-Bt}-1) \tag{34}$$

where

$$A=(k_{\mathrm{tr}}+k_{\mathrm{p}})M,\quad B=k_{\mathrm{tr}}M+k_{\mathrm{d}} \tag{35}$$

So the number-average and weight-average molecular weights of polymer can be calculated from

$$\overline{M_{\mathrm{n}}}=\frac{S_1}{S_0}M_{\mathrm{e}};\quad \overline{M_{\mathrm{w}}}=\frac{S_2}{S_1}M_{\mathrm{e}} \tag{36}$$

where $M_{\mathrm{e}}$ is the molecular weight of ethylene.

For the case of a multiple active sites system all reactions and equations described above for a single site system are still workable with the addition of the subscript $i$ indicating the types of active site.

So, the following equations can be obtained.

$$C_i=C_{i,0}\,\mathrm{e}^{-k_{\mathrm{d}_i}t}\quad i=1,\ 2,\ \ldots,\ n \tag{37}$$

$$C=\sum C_{i,0}\,\mathrm{e}^{-k_{d_i}t} \tag{38}$$

$$R_{\mathrm{p}_i}=k_{\mathrm{p}_i}MC_{i,0}\,\mathrm{e}^{-k_{\mathrm{d}_i}t} \tag{39}$$

$$R_{\mathrm{p}}=\sum k_{\mathrm{p}_i}MC_{i,0}\,\mathrm{e}^{-k_{\mathrm{d}_i}t} \tag{40}$$

$$P_i=\int k_{\mathrm{p}_i}MC_i\,\mathrm{d}t=k_{\mathrm{p}_i}MC_{i,0}/k_{\mathrm{d}_i}(1-\mathrm{e}^{-k_{\mathrm{d}_i}t}) \tag{41}$$

$$P=\sum P_i=\sum k_{\mathrm{p}_i}MC_{i,0}/k_{\mathrm{d}_i}(1-\mathrm{e}^{-k_{\mathrm{d}_i}t}) \tag{42}$$

$$\overline{M_{\mathrm{n}_i}}=\frac{S_{i,1}}{S_{i,0}}M_{\mathrm{e}} \tag{43}$$

$$\overline{M_{\mathrm{n}}}=\frac{\sum S_{i,1}}{\sum S_{i,0}}M_{\mathrm{e}} \tag{44}$$

$$\overline{M_{\mathrm{w}_i}}=\frac{S_{i,2}}{S_{i,1}}M_{\mathrm{e}} \tag{45}$$

$$\overline{M_{\mathrm{w}}}=\frac{\sum S_{i,2}}{\sum S_{i,1}}M_{\mathrm{e}} \tag{46}$$

### 3.4. Parameter estimation

The types of active site, the molecular weight ($M_{\mathrm{n}_i}$ and $M_{\mathrm{w}_i}$) and fraction of components $F_i$ produced by each site can be estimated by fitting the GPC curves with the multiple Flory-distribution equation [6]:

$$H(W)=\sum K_ia_i\exp\{4.6\log(n)-a_i\exp[2.3\log(n)]\} \tag{47}$$

where $H(W)$ is weight distribution function, $n$ is the polymerization degree, $a_i$ is the probability of the chain termination reaction and the average polymerization degree $\bar{n}$ of the polymers is equal to $1/a_i$, $K_i$ is a coefficient related to the areas for different $a_i$ values. The fitting results are shown in Tables 1 and 2.

Since the consumption of ethylene was measured during the polymerization, the consumption rate given in Eq. (42) instead of the polymerization rate from Eq. (40) was chosen for estimation of the parameters $k_{\mathrm{d}_i}$ and $(k_{\mathrm{p}_i}C_{i,0})$ which may prevent introducing errors from the differentiation calculation.

For Eq. (41) when $t=t_{\mathrm{f}}$, the productivity of each active site is

$$P_i(t_{\mathrm{f}})=D_i(1-\mathrm{e}^{-k_{\mathrm{d}_i}t_{\mathrm{f}}})=WF_i \tag{48}$$

where $D_i=k_{\mathrm{p}_i}MC_{i,0}/k_{\mathrm{d}_i}$, $W$ is the whole productivity and $t_{\mathrm{f}}$ is the total time of polymerization.

Eq. (48) can be solved to give

$$k_{\mathrm{d}_i}=-\ln[1-(WF_i/D_i)]/t_{\mathrm{f}} \tag{49}$$

The cumulative productivity can be described by combining

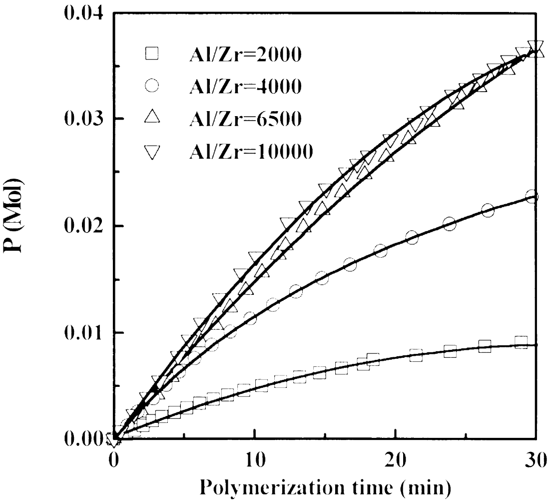

Fig. 7. Variation of cumulative productivity with time for $Cp_2ZrCl_2$–MAO using different Al/Zr ratios (dots: measured; lines: fitted with MSmodel).

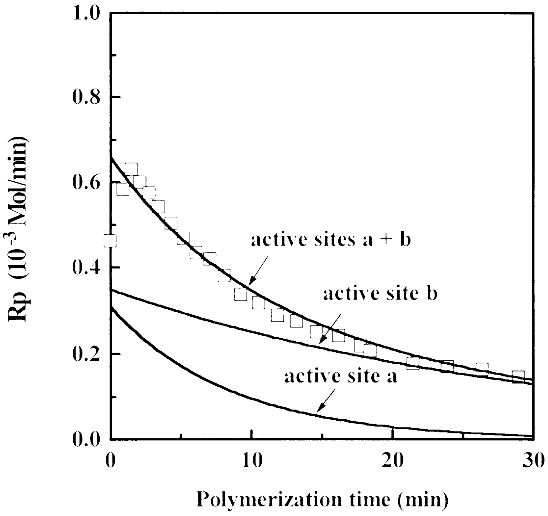

Fig. 8. Polymerization rate of ethylene for $Cp_2ZrCl_2$–MAO (Al/Zr = 2000; dots: tested; lines: prediction of two sites and their sum).

Eqs. (42) and (49), which yields

$$P(t) = \sum D_i \left\{ 1 - \exp\left[ \frac{\ln\left(1 - \frac{WF_i}{D_i}\right)}{t_f} t \right] \right\} \qquad (50)$$

It is convenient to use Eq. (50) for fitting because there is only one type of parameter. A non-linear regression method based on the Levenberg–Marquardt algorithm for non-linear least-squares analysis was employed to fit Eq. (5) to the measured polymerization rate data. The results are illustrated in Figs 7 and 8. From fitting, the parameters $D_i$ can be obtained directly and then $k_{d_i}$ can also be calculated using Eq. (49).

The parameters $k_{tr_i}$, $k_{p_i}$ and $C_{i,0}$ were finally obtained by fitting Eqs. (43) and (45) to the molecular weight of components resolved by the Flory equation.

Tables 3 and 4 show the total results of fitting with the MSmodel.

## 4. Results and discussion

With the help of a computer, the ethylene polymerization was simulated with the MSmodel proposed in this paper for MAO and BAO systems. The close agreements, not only between the experimental and fitted profiles, $M_n$ and $M_w$ values, but also the fractions of each component, are indications of the validity of the MSmodel.

One feature of the homogeneous metallocene catalyst is that it has a definite structure and simple active species, so the polymers produced by metallocenes are characterized by their narrow MWD. However, some studies have shown that the molecular distribution of the polymer produced by metallocenes is either a wide or a bimodal distribution [5] under certain polymerization conditions. The answer to this fact is that the metallocene possessed simple sites instead of a single active site. Based on this understanding some experimental results can be explained.

In the $Cp_2ZrCl_2$–MAO catalyst system there are two types of active site, one site (site ‘‘a’’) produces the

Table 3
Kinetic parameter estimates for ethylene polymerization with $Cp_2ZrCl_2$–MAO[a]

| Al/Zr | $M_n \times 10^{-4}$ (g mol$^{-1}$) | $C_0$ ($10^{-7}$ mol) | $k_p \times 10^{-4}$ (M$^{-1}$ min$^{-1}$) | $k_d$ (min$^{-1}$) | $k_{tr}$ (M$^{-1}$ min$^{-1}$) | Wt% |
|---|---|---|---|---|---|---|
| 2000 | 29.6 | 0.14 | 30.4 | 0.033 | 28.7 | 73 |
| | 9.0 | 0.87 | 4.45 | 0.13 | 12.3 | 27 |
| 4000 | 32.6 | 0.21 | 33.6 | 0.031 | 28.5 | 79 |
| | 9.99 | 0.80 | 7.76 | 0.14 | 25.9 | 21 |
| 6500 | 42.4 | 0.32 | 44.4 | 0.033 | 28.8 | 63 |
| | 12.0 | 0.64 | 12.5 | 0.033 | 28.7 | 37 |
| 10 000 | 44.9 | 0.35 | 45.7 | 0.035 | 27.9 | 64 |
| | 12.2 | 0.71 | 12.5 | 0.035 | 27.9 | 36 |

[a] Polymerization conditions same as Fig. 1.

Table 4
Kinetic paramter estimates for ethylene polymerization with $Cp_2ZrCl_2$–BAO[a]

| Al/Zr | $M_n \times 10^{-4}$ (g $mol^{-1}$) | $C_0$ ($10^{-7}$ mol) | $k_p \times 10^{-4}$ ($M^{-1}$ $min^{-1}$) | $k_d$ ($min^{-1}$) | $k_{tr}$ ($M^{-1}$ $min^{-1}$) | Wt% |
|---|---|---|---|---|---|---|
| 5000 | 33.2 | 0.23 | 5.15 | 0.05 | 3.53 | 49 |
| | 8.7 | 0.48 | 1.35 | 0.05 | 3.58 | 28 |
| | 1.9 | 2.28 | 0.29 | 0.06 | 3.19 | 23 |
| 7000 | 28.0 | 0.69 | 4.42 | 0.04 | 3.66 | 50 |
| | 9.2 | 1.22 | 1.54 | 0.04 | 3.66 | 31 |
| | 2.1 | 2.95 | 0.40 | 0.04 | 3.66 | 19 |
| 8000 | 28.0 | 0.99 | 4.41 | 0.04 | 3.65 | 57 |
| | 9.8 | 1.49 | 1.44 | 0.04 | 3.65 | 28 |
| | 2.5 | 3.62 | 0.33 | 0.04 | 3.65 | 15 |

[a] Polymerization conditions same as Fig. 2.

polymers with low molecular weight and the other site (site ‘‘b’’) produces the high molecular weight polymers. When the Al/Zr ratio increases, the reaction constant $k_p$ for both sites increases, the $k_d$ and $k_{tr}$ of site ‘‘b’’ change very little whereas the $k_d$ of site ‘‘a’’ decreases and $k_{tr}$ increases rapidly. For a high Al/Zr ratio (Al/Zr = 10 000) the reaction constants of both sites remain unchangeable with different $k_p$. So it is concluded that an increase of MAO mainly improves the stability and $k_p$ of the low molecular weight center (site ‘‘a’’).

For the mechanism of formation of active centers, Chien and Wang [4] proposed that the metallocene can be coordinated to zero, one, or two MAOs, resulting in active centers of different $k_p$. We also consider that the formation of multiple active sites can be attributed to interaction between metallocene and aluminoxane. Furthermore, we think there must be a maximum number of coordinated aluminoxane owing to steric effects and a minimum number owing to the stability of the center. This assumption is derived from the coordination of metal ions with organic ligands. So the number of centers having polymerization ability must lie between the minimum and maximum number. There is an equilibrium among the different active centers which may be influenced by the amount of MAO.

The change of Al/Zr affects not only the kinetic parameters, polymerization rate and average molecular weight, but also the variation of polydispersity during the polymerization. Fig. 9 shows the variations of polydispersity for two Al/Zr ratios predicted using the two active sites MSmodel. For the case of Al/Zr = 2000 the maximum polydispersity is reached within a few minutes and followed by a gentle decrease. When the Al/Zr ratio is 6500 the polydispersity increases rapidly within the first few minutes and still increases gradually with the polymerization time. Fig. 10 shows the variation of polydispersity for different Al/Zr ratios for the $Cp_2ZrCl_2$–MAO catalyst reported by Chien and Wang [4], which confirms the prediction by the MSmodel proposed in this paper. This is further evidence of the validity of the MSmodel. The exact answer to the

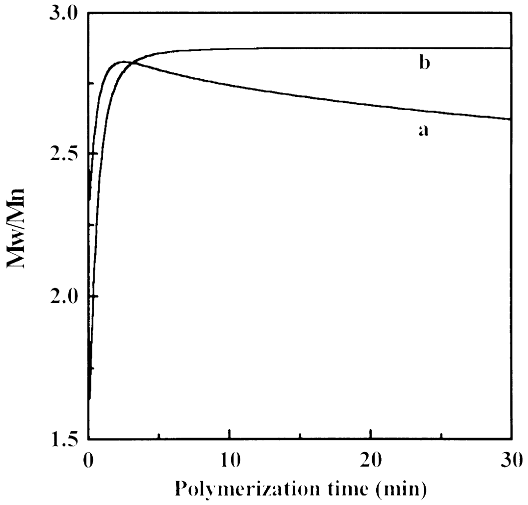

Fig. 9. Prediction of variation of $M_w/M_n$ versus polymerization time: (a) Al/Zr = 2000; (b) Al/Zr = 6500.

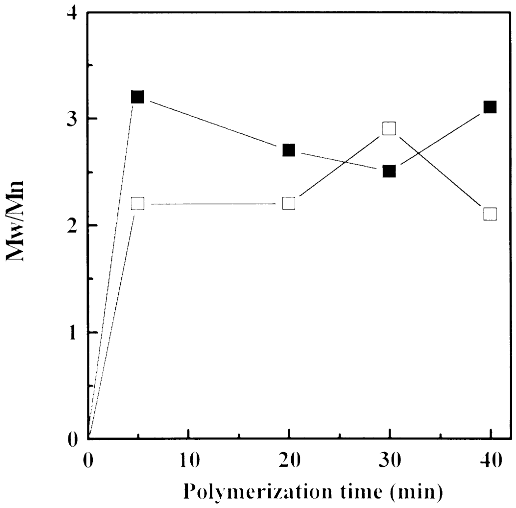

Fig. 10. Variation of $M_w/M_n$ versus polymerization time of $Cp_2ZrCl_2$–MAO reported by Chien and Wang [4] (■, Al/Zr = 1070; □, Al/Zr = 10 800).

variation is there are two types of active site with different $k_d$ values.

Fitting the polymerization profiles of the BAO system with the MSmodel also led to good agreement. The result has already been given in Table 4. Since there was a short build-up period for the BAO system, a less close agreement was achieved. The variation of estimated parameters with Al/Zr ratio is similar to the MAO systems. It is noteworthy that the fitted value of active sites was less than the metallocene amount. A reasonable explanation is that the conversion of catalyst in the BAO system is low because of its low cocatalyst ability. The answer may also explain the low catalytic activity for BAO compared with MAO.

The estimated parameters for polymerization based on combining $Cp_2ZrCl_2$ with different aluminoxanes under approximate Al/Zr ratios (Al/Zr = 4000 for MAO and Al/Zr = 5000 for BAO) were compared. The conversion of metallocene to active species for both types of aluminoxane is quite different. For MAO the conversion is approximately 100%, whereas for BAO it is only 30%. The reason for the diversity may be attributed to their various cocatalytic abilities, including alkylation ability and stability of active species. Because MAO posses the strongest alkylation ability and can also stabilize the cation active site, nearly all the metallocene can be transformed into active species. For the case of BAO, its alkylation ability is weak compared with MAO and this leads to a low conversion. The reaction constant $k_{tr}$ of BAO is smaller than that of MAO, which may be due to the steric effect of the *iso*-butyl group preventing the interaction between the $\beta$-hydrogen atom and the metal center which leads to a $\beta$-hydrogen elimination transfer reaction.

## 5. Conclusions

Based on the kinetics studies of ethylene polymerization with $Cp_2ZrCl_2$ with different aluminoxanes and analysis of GPC curves of polymers using the Flory-distribution equations, it is concluded that there are multiple active sites in the metallocene catalytic system. A multiple active sites kinetic model (MSmodel) was proposed for ethylene polymerization. Good agreements of polymerization rate and variation of polydispersity were achieved for fitting the kinetic profiles using the MSmodel. The difference between the estimated parameters of the two aluminoxanes was discussed and explained in detail.

## Acknowledgements

Financial support by the National Natural Science Foundation of China (No 29474170) is gratefully acknowledged.

## References

[1] Kaminsky W, Bark A, Speihl R, Moller-Lindenhof N, Niedoba S. In: Kaminsky W, Sinn H, editors. Transition metals and organometallics as catalyst for olefin polymerization. Berlin: Springer, 1988:291.

[2] Kaminsky W, Schlobohm M. Makromol Chem Mackromol Symp 1986;4:103.

[3] Schmidt GF. In: Quirk RP, editor. Transition metal catalyzed polymerization. Cambridge: Cambridge University Press, 1988:151.

[4] Chien JCW, Wag BP. J Polym Sci Polym Chem 1990;28:15.

[5] Estrada JMW, Hamielec AE. Polymer 1994;35:808.

[6] Kissin YV. J Polym Sci Polym Chem 1995;33:227.